GEOPHYSICS, VOL. 68, NO. 5 (SEPTEMBER-OCTOBER 2003); P. 1503–1509, 5 FIGS., 1 TABLE.
10.1190/1.1620623

An inclusion-based model of elastic wave velocities incorporating patch-scale fluid pressure relaxation

S. Richard Taylor* and Rosemary J. Knight‡

ABSTRACT

We consider elastic wave velocities in fluid-saturated porous media with pore fluids distributed in "patches" (i.e., heterogeneity much larger than the typical pore size). We model elastic properties of such materials using inclusion-based effective medium theory (IBEMT). The standard IBEMT formulation assumes insufficient time during the wave cycle for pore fluids to flow in response to wave-induced pressure gradients. Our approach accounts for this flow, incorporating wave-frequency dependent flow effects in the definition of effective elastic moduli for patches. Effective moduli are used in conjunction with IBEMT to estimate elastic moduli of the composite material. In the low- and high-frequency limits, the model reproduces previous theoretical results. At intermediate frequencies, it yields results qualitatively similar to other patch-scale models. We demonstrate this approach, estimating elastic P-wave velocities and attenuation in a porous rock that simultaneously contains fluid-saturated patches of different sizes.

INTRODUCTION

There is substantial evidence from laboratory experiments (Knight and Nolen-Hoeksema, 1990; Cadoret et al., 1995) and theoretical models (White, 1975; Endres and Knight, 1989; Gist, 1994; le Ravalec et al., 1996) that elastic wave velocities in fluid-saturated porous media can depend strongly on the spatial distribution of pore fluids. In particular, it has been observed (in the experimental studies referenced above) that a porous medium in which the fluids are distributed heterogeneously is typically less compliant, and exhibits higher elastic wave velocities, than the same medium with a more homogeneous distribution of pore fluids. To accurately model wave velocities over the range of frequencies of interest to the geophysical community, it is important to account for this effect.

In fluid-saturated porous media, two distinct scales of fluid distribution are typically identified: the pore scale and the "patch" scale. In the literature, the term "patch" is used for scales above the pore scale. This includes, for example, saturation heterogeneity at the centimeter-scale in laboratory samples, and saturation heterogeneity at the scale of meters (or more) in the subsurface. For each scale of heterogeneity, there is a characteristic time scale of fluid pressure relaxation, τ, that determines the elastic response at a given wave frequency (e.g., Dvorkin et al., 1994). Consider, for example, a liquid/gas-saturated medium in which fully liquid-saturated regions (patches) are adjacent to fully gas-saturated regions. When the medium is deformed by a passing elastic wave, the induced fluid pressure is initially heterogeneous and therefore provides elastic reinforcement to the solid matrix. If the wave period is much greater than τ, flow from liquid-saturated patches to the gas-saturated regions will equilibrate (or relax) the fluid pressure between macroscopic regions, thereby limiting the extent to which the liquid reinforces the matrix. In the other extreme, where the wave period is much less than τ, there is insufficient time for significant relaxation. The patches are then undrained, the liquid being effectively trapped within each patch, and elastic reinforcement by the liquid is maximized.

A number of approaches have been proposed for modeling the effects of patch-scale saturation heterogeneity. Le Ravalec et al. (1996) treat distinct macroscopic patches as elastic inclusions within a background matrix. An inclusion-based effective medium theory (IBEMT) (le Ravalec and Guéguen, 1996) is then used to estimate the effective elastic moduli, and hence the elastic wave velocities for the composite. Since the IBEMT assumes that hydraulic communication between inclusions does not occur (i.e., inclusions are undrained), this approach models the high-frequency, or unrelaxed, response of the composite. A similar approach to the undrained case (Knight et al., 1998), employs the Hashin-Shtrikman bounds on elastic moduli rather than an inclusion-based theory.

The "gas pocket" model of White (1975), with a correction by Dutta and Seriff (1979), treats the full frequency range

Manuscript received by the Editor August 16, 1999; revised manuscript received February 18, 2003.
*University of Waterloo, Department of Applied Mathematics, Waterloo, Ontario N2L 3G1, Canada. E-mail: sr2taylo@math.uwaterloo.ca.
‡Stanford University, Mitchell Building, Geophysics Department, Stanford, California 94305-2215. E-mail: rknight@pangea.stanford.edu.

accessible to effective medium theory. This model assumes an idealized fluid distribution in which a cubic array of spherical gas-saturated patches is embedded in an otherwise liquid-saturated medium. White estimates the effective elastic moduli for this medium, accounting for flow between liquid- and gas-saturated regions. Dutta and Odé (1979) provide a more rigorous solution of White's model, incorporating Biot's (1956) equations of poroelasticity. While it is able to treat the full frequency response of a porous composite with patchy saturation, the White model is limited compared to IBEMT. In particular, White allows for only a single length scale of heterogeneity, rather than a range of simultaneous patch sizes. Furthermore, the inclusion-based approach includes a variety of inclusion geometries, whereas White treats only spherical patches.

The purpose of the present work is to further develop IBEMT to model patch-scale saturation heterogeneity across a wide frequency range. In particular, we remove the assumption (usually included in IBEMT models) that the inclusions are undrained. We accomplish this by using complex elastic moduli, which describe both the elastic and dissipative components of the response to sinusoidal deformation (e.g., Berryman, 1980a, b). We model the viscoelastic response of a fluid-saturated patch, accounting for pressure relaxation, by deriving an expression for the (complex) effective bulk modulus of the patch. With the introduction of this effective modulus, we treat the dynamic response of the patch to sinusoidal deformation within an IBEMT computation of the elastic properties of the composite. This permits us to model the full frequency range treated by White (1975), while retaining the advantages of the IBEMT approach.

MODEL

We consider an idealized unit cell in a fluid-saturated porous medium, consisting of a spherical region of radius a (the "patch", denoted as region 1), enclosed at the center of a sphere of radius $b > a$ (region 2). Both regions are assumed to be completely saturated with different fluids. This situation, illustrated in Figure 1, is considered by White (1975). As in White, the outer radius, b, is chosen to obtain the same global volumetric proportions of the two fluids as in the medium being modeled. That is, if the porosity in the two regions is identical, then a and b are related by $S_1 = a^3/b^3$, where S_1 is the global level of saturation with the fluid in region 1.

Within each region all material properties (e.g., porosity, permeability, etc.) are spatially uniform. Also, the porosity within each region is homogeneous, in that a uniform applied pressure field will induce a uniform fluid pressure. We allow that the material properties may change across the patch boundary, which is consistent with the expectation that heterogeneity of the fluid distribution coincides with heterogeneity of the underlying lithology. These assumptions are the same as White's.

In Appendix A, we derive a diffusion equation governing the evolution of the fluid pressure, p_f, induced by a passing elastic wave. We obtain

$$\frac{\partial p_f}{\partial t} = D_p \nabla^2 p_f + \frac{\alpha F_p}{\phi \kappa_d} \frac{\partial p}{\partial t}, \tag{1}$$

where p is the applied pressure field, ϕ is the porosity, κ_d is the drained bulk modulus of the porous matrix, and $\alpha = 1 - \kappa_d/\kappa_s$ is commonly referred to as the "poroelastic parameter," where κ_s is the bulk modulus of the mineral solid. D_p and F_p are functions of the material properties and are defined in the Appendix A. Equation (1) describes the relaxation of fluid pressure (via the diffusive term $\nabla^2 p_f$) from flow due to the forcing term, p.

Under the effective medium assumption, the elastic wavelength is much greater than the length scale of heterogeneity (i.e., the unit cell size, b), so we approximate the pressure field p to be uniform. Denoting the angular frequency of the incident wave by $\omega = 2\pi f$, where f is the wave frequency in hertz, we represent the pressure field as $p(t) = p_0 e^{i\omega t}$. Similarly writing the overall volumetric dilatation of the patch as $\theta(t) = \theta_0 e^{i\omega t}$, we can solve the diffusion equation (1) and obtain a relation of the form

$$p_0 = -\kappa^* \theta_0. \tag{2}$$

This defines the effective bulk modulus of the patch, κ^*. That is, the viscoelastic response of the patch to sinusoidal deformation is identical to that of an equivalent homogeneous medium with bulk modulus κ^*. In general, κ^* will be a complex number, reflecting that the stress and dilatation fields will be out of phase as a result of fluid flow.

The solution of the diffusion equation (1), and isolation of the parameter κ^* in terms of material properties and the wave frequency, is shown in detail in Appendix B, where we obtain the expression

$$\kappa^* = \frac{\kappa_{d(1)}}{1 - \alpha_1 [G_1 + F(\omega)(G_2 - G_1)]}. \tag{3}$$

To compute elastic properties of a porous composite, we used equation (3) to estimate effective elastic moduli for all patches, and apply an inclusion-based effective medium theory to estimate elastic moduli for the composite (Berryman, 1980a, b). We model the "nonpatch" region by unsaturated

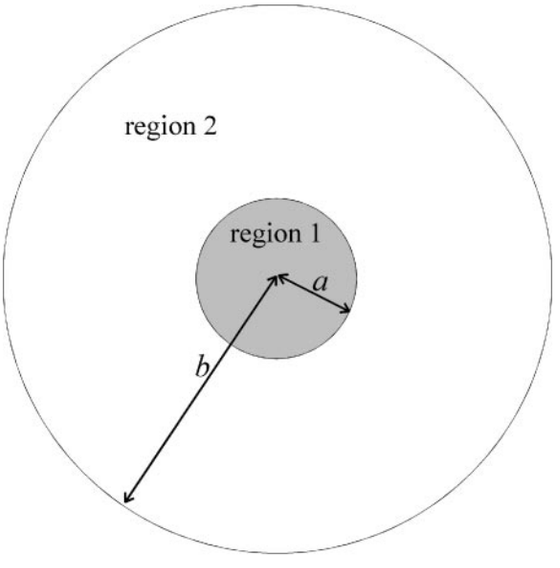

FIG. 1. Idealized model of a spherical fluid-saturated patch of radius a (region 1), embedded in a spherical porous background of radius b (region 2) saturated with a different fluid. [After Figure 1 of White (1975).]

spherical patches to estimate the effects of fluid pressure relaxation on the effective bulk modulus of this region. For example, in a medium with spherical liquid-saturated patches in a gas-saturated background, we use equation (3) to compute effective elastic moduli for both the water- and gas-saturated regions. While this approach is only approximate, it permits one to treat the two regions in a symmetric way, without regard for which fluid is to be regarded as "patchy."

For a medium saturated with two fluids, we expect that the length scales, a_1 and a_2, associated with regions saturated with fluids 1 and 2, respectively, will be approximated by

$$\frac{a_1}{a_2} = \frac{S_1}{S_2}, \tag{4}$$

where S_1 and S_2 are the global levels of saturation with each fluid. Accordingly, we use this equation to relate the radii, a_1 and a_2, of the patches used to represent each region. For patches of multiple sizes or fluid types, we generalize this expression to

$$\frac{a_1}{S_1} = \ldots = \frac{a_i}{S_i} = \ldots, \tag{5}$$

where a_i is the radius of patches used to approximate the ith region (fluid type or patch size), which occupies the fractional volumetric proportion S_i.

Frequency response of a Patch

Dvorkin et al. (1994) show that the characteristic timescale of pressure diffusion, τ, out of a patch of radius a is given by $\tau \approx a^2/D_p$ where D_p is the pressure diffusivity, defined in Appendix A. This timescale provides an estimate of the characteristic wave frequency, $f_0 = 1/\tau$, near the transition from the drained to the undrained response as frequency increases. An attenuation peak associated with a maximum rate of viscous dissipation due to fluid flow is also expected near this characteristic frequency. The model developed here is also governed by this characteristic frequency [cf., equation (B-9)], along with a characteristic frequency associated with pressure diffusion within the region surrounding a patch [cf., equation (B-15)].

We characterize the full frequency response of a patch by the frequency-dependent effective bulk modulus given by equation (3). To illustrate the form of this frequency response, Figure 2 shows the real and imaginary parts of the effective bulk modulus, κ^*, versus the scaled frequency, $a^2 f$, for a water-saturated patch imbedded in a sandstone that is otherwise saturated with air, at 12.5% water saturation ($a/b = 0.5$). We have scaled the wave frequency by a^2 since it can be seen in Appendix B that the frequency and patch size enter only through the term $a^2 f$, and we can therefore use a single curve to represent the response for all patch sizes. The corresponding material data are given in Table 1. We observe the expected qualitative behavior, with the real part of the bulk modulus increasing along a sigmoid curve as the frequency is increased. The transition between the low- and high-frequency limits occurs near the characteristic relaxation frequency, where $f \approx 1/\tau$. The imaginary part of κ^* (which represents the stress in the patch that is out of phase with the dilatation, and is associated with viscous dissipation caused by fluid flow) exhibits a peak near the relaxation frequency, and goes to zero in the low- and high-frequency limits. In these limits, the pressure and dilatation within the patch are in phase. Note that the transition from low- to high-frequency behavior is very gradual, occurring over more than three frequency decades. The response is also asymmetric about the characteristic relaxation frequency. These aspects of the frequency response are markedly different from that of the standard linear solid commonly used to model viscoelastic behavior (e.g., Mavko et al., 1998, 197).

EXAMPLE: MULTIPLE SCALES OF HETEROGENEITY

In porous rock, heterogeneity exists at a wide range of scales, from pores (on the order of micrometers) to lithologic variation (on the order of meters or greater). Our model does not provide a fully consistent framework for treating multiple simultaneous

Table 1. Physical parameters for Spirit River sandstone saturated with water and gas.

Parameter	Numerical Value
Porous matrix (Spirit River sandstone)	
Dry-frame bulk modulus, κ_d [GPa]	5.6*
Dry-frame shear modulus, μ_d [GPa]	12.6*
Porosity, ϕ	0.052‡
Permeability, K [μD]	1‡
Mineral solid (quartz)	
Bulk modulus, κ_s [GPa]	38**
Density, ρ_s [kg/m^3]	2630**
Water	
Bulk modulus, κ_{water} [GPa]	2.2
Viscosity, η_{water} [10^{-3} Pa · s]	1
Density, ρ_{water} [kg/m^3]	1000
Gas	
Bulk modulus, κ_{gas} [MPa]	0.8
Viscosity, η_{gas} [10^{-3} Pa · s]	0.05
Density, ρ_{gas} [kg/m^3]	100

*Estimated from velocity measurements by Knight and Nolen-Hoeksema (1990).
‡From Knight and Nolen-Hoeksema (1990).
**From le Ravalec et al. (1996).

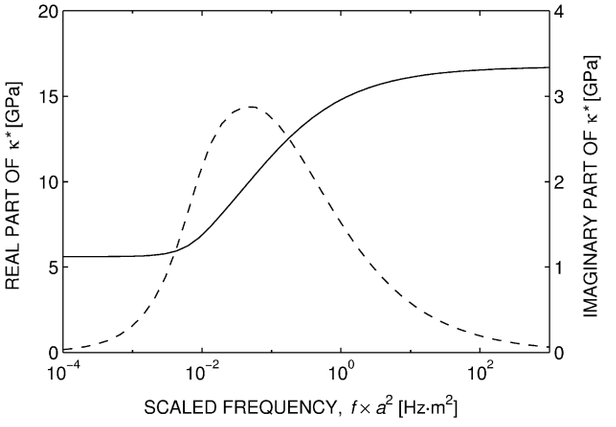

FIG. 2. Computed real (solid line) and imaginary (dashed line) parts of the effective bulk modulus, κ^* [equation (3)], versus the scaled wave frequency, $a^2 f$, for a water-saturated patch of radius a embedded in a gas-saturated sandstone, using the model developed here. The corresponding material data are given in Table 1. This illustrates the general form of the frequency-response of a fluid-saturated patch, as well as the dependence on patch size.

scales of heterogeneity (where the treatment is complicated by successively smaller scales of heterogeneity, which may be embedded within larger patches); it does provide insight into the qualitative behavior of such materials.

Consider an instance in which the fluids saturating a porous rock occur in patches having a range of distinct sizes. There will be a frequency threshold above which the pore fluids can be regarded as completely unrelaxed (i.e., above which flow caused by wave-induced pressure gradients is negligible). In this case the model of Knight et al. (1998) can be used to estimate elastic velocities for the composite. As the wave frequency decreases below this threshold, the wave period will be sufficiently long for fluid pressure relaxation to occur across the smallest length scale of heterogeneity. It is the smallest scale of heterogeneity that is the first to relax because the distance over which fluid pressures must diffuse is the shortest. This relaxation weakens the elastic response of the composite, and there is an associated decrease in the wave velocities.

If the wave frequency is decreased further, the wave period eventually becomes sufficiently long that fluid pressure differences between neighboring patches of the next greater size have sufficient time to relax. In this way, a sequence of relaxations occurs as the characteristic frequency (proportional to $1/a^2$) corresponding to each successive length scale of heterogeneity, a, is traversed. When the wave frequency becomes sufficiently low that the fluid pressure is completely relaxed at the largest scale of heterogeneity, Gassmann's (1951) formulas for the elastic moduli of the composite become valid.

The model developed in the previous section applies in the situation just described. We illustrate this by considering the particular example of a water/gas-saturated porous rock in which the water is present in distinct spherical patches of diameter 5 mm and 5 cm. The resulting P-wave velocity and attenuation versus wave frequency are shown in Figure 3. We have used the material properties given in Table 1, and assumed that the medium is 80% water saturated, with the water being distributed in equal volumetric proportions between the larger and smaller patches. We used the patch-scale relaxation model to estimate effective elastic moduli for the patches, and applied Berryman's (1980a, b) IBEMT to estimate effective elastic moduli for the composite, for wave frequencies ranging from 1 Hz to 1 MHz. The velocity and attenuation curves shown in the figure demonstrate two successive relaxations that occur as the wave frequency is decreased from the completely unrelaxed limit to the completely relaxed limit. First the smaller patches relax as the frequency decreases between 10^3 and 10^4 Hz (where there is a distinct drop in P-wave velocity as well as a peak in attenuation), then the larger patches relax as the frequency decreases further between 10^1 and 10^2 Hz (where there is again a drop in P-wave velocity and a peak in attenuation). It is interesting to note that if patch-scale heterogeneity exists at sufficiently many scales, the Q_p^{-1} versus frequency curve of Figure 3 approaches a straight line, corresponding to the "constant Q^{-1}" model.

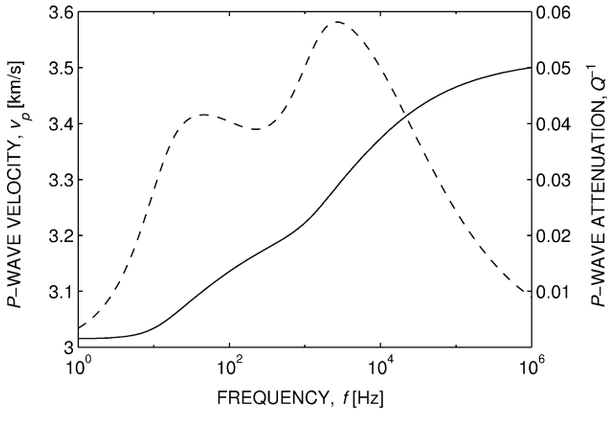

FIG. 3. Computed elastic P-wave velocity (solid line) and attenuation (dashed line) versus wave frequency for a typical water- and gas-saturated sandstone at 80% water saturation, in which the water is distributed in equal volumetric proportions between spherical patches of diameter 5 mm and 5 cm. The corresponding material data are given in Table 1.

DISCUSSION

In the low-frequency limit, the wave-induced fluid pressures equilibrate throughout the pore fluids. In this case, under the simplifying assumption that the porosity is uniform, equation (3) for the effective bulk modulus simplifies to

$$\kappa^* = \kappa_d + \frac{\alpha^2}{\dfrac{\phi}{\kappa_f^{\text{eff}}} + \dfrac{\alpha - \phi}{\kappa_s}} \quad (\omega \to 0). \tag{6}$$

The "effective fluid" bulk modulus, κ_f^{eff}, is the Reuss average over the fluid components:

$$\frac{1}{\kappa_f^{\text{eff}}} = \frac{S_1}{\kappa_{f(1)}} + \frac{S_2}{\kappa_{f(2)}}, \tag{7}$$

where $S_1 = a^3/b^3$ and $S_2 = 1 - S_1$ are the global of saturations with respect to fluids 1 and 2, respectively. Equation (6) reproduces Gassmann's (1951) formula for the bulk modulus of an undrained medium, modified to account for the presence of multiple fluid components (Domenico, 1977). Thus, in the low-frequency limit, our model agrees with Gassmann's relations, and therefore also with the low-frequency limit of the corrected White model (White, 1975; Dutta and Seriff, 1979).

In the high-frequency limit, where there is insufficient time during a wave cycle for flow to lead to pressure equilibration, a fluid-saturated patch behaves as an undrained, hydraulically isolated system. In this limit, we have $F(\omega) \to 0$ in equation (3), and we obtain

$$\kappa^* = \kappa_{d(1)} + \frac{\alpha_1^2}{\dfrac{\phi_1}{\kappa_{f(1)}} + \dfrac{\alpha_1 - \phi_1}{\kappa_{s(1)}}} \quad (\omega \to \infty). \tag{8}$$

This reproduces Gassmann's relation for the effective bulk modulus of an undrained region saturated with fluid 1. In Knight et al. (1998), this equation is used to estimate elastic moduli of individual patches, assuming that the patches behave as undrained systems, and IBEMT is used to estimate wave velocities for the composite. Thus our approach improves on Knight et al. in that our model reduces to theirs in the high-frequency limit, but also treats lower frequencies since we do not assume that patches are hydraulically isolated.

As in Knight et al. (1998), we have made the somewhat restrictive assumption of homogeneous porosity, which further requires that the pore fluids be homogeneously distributed

within each macroscopic patch. Thus neither model can account for the effects of pore-scale fluid distribution, which are known to be significant (Endres and Knight, 1989). The inclusion-based model of le Ravalec et al. (1996) overcomes this limitation and accounts for the simultaneous effects of pore- and patch-scale saturation heterogeneity. However, their model is applicable only when fluid pressures at all scales of heterogeneity are unrelaxed.

The geometrical construction of our model is very similar to that of White (1975). Thus, we expect the results of the two models to agree closely when applied in the same modeling situation. Indeed, we have shown above that the two models are identical in the low-frequency limit of complete relaxation. However, direct analytical comparison across the full range of frequencies is not possible: the model presented here provides an expression for the effective properties of a patch only. The IBEMT used to estimate the properties of the composite medium is a separate component of the model and has been left unspecified. This flexibility is not provided by the White approach, where the effective medium theory is an inherent part of the model and effective properties of the composite (rather than individual patches) are computed directly.

To permit comparison of the two approaches on the same basis, we compute effective properties of an idealized medium using our inclusion-based model, together with a particular IBEMT (Berryman, 1980a, b), and compare the results graphically with those obtained using the White model. Figures 4 and 5 show the resulting P-wave velocity and attenuation versus wave frequency, as computed using both the White model and the inclusion-based model developed here. The model medium, detailed in Table 1, is a typical sandstone saturated with water and gas, in which the gas exists in spherical patches of radius 1 cm. The figure compares various levels of gas saturation. Note that the two models agree very closely in both velocity and attenuation, particularly at high levels of water saturation. Thus we conclude that the model presented here generalizes the White model within an inclusion-based framework.

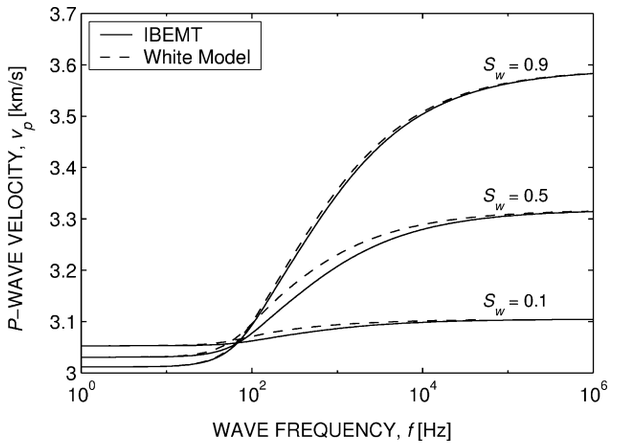

FIG. 4. Computed elastic P-wave velocity versus wave frequency for a water- and gas-saturated sandstone at various levels of water saturation, in which the water is distributed in patches of radius 1 cm. For comparison, results are shown both for the inclusion-based model developed here (solid line) and for the White (1975) model (dashed line). It can be seen that the two models agree closely. The corresponding material data are given in Table 1.

Dutta and Odé (1979) have solved the White model more rigorously, using Biot's (1956) equations of poroelasticity rather than an effective medium approach. They obtain results that agree closely with those of White, but are also able to account for the inertial effects of solid-fluid coupling. In particular they have identified the role of the Biot slow wave in the model. The Dutta and Odé solution is clearly more sophisticated than ours in this respect. The present model relies on an effective medium theory to estimate elastic properties of the fluid-saturated composite, and consequently is unable to account for inertial phenomena such as the Biot slow wave. Nevertheless, many limitations of the White model—including the requirement of a single scale of heterogeneity and the restriction to spherical geometry—are retained in the solution by Dutta and Odé. The IBEMT approach advocated here does not rely on these assumptions, and as such is a more versatile approach in situations where the effective medium approximation is valid.

CONCLUSION

IBEMT is a well-established and convenient framework for modeling the elastic properties of heterogeneous materials such as porous rock with patch-scale heterogeneity. However, in its standard formulation, IBEMT precludes hydraulic interaction between distinct regions of the pore space. This has limited previous IBEMT models to situations where relaxation of fluid pressure does not occur (due to sufficiently large patches, high frequency, or low permeability).

We have shown that it is possible to eliminate these limitations of IBEMT by replacing a fluid-saturated patch with an equivalent elastic inclusion whose frequency-dependent bulk modulus models the effects of fluid pressure relaxation. To illustrate this approach, we have derived an expression for the effective bulk modulus of a spherical patch, based on a model similar to that of White (1975). In the high-frequency limit, the resulting IBEMT model reduces to the model of Knight et al. (1998), in the low-frequency limit, it reproduces Gassmann's (1951) low-frequency relations appropriately modified to account for multiple fluid phases (Domenico, 1977). However, the most important feature of the model is that for intermediate

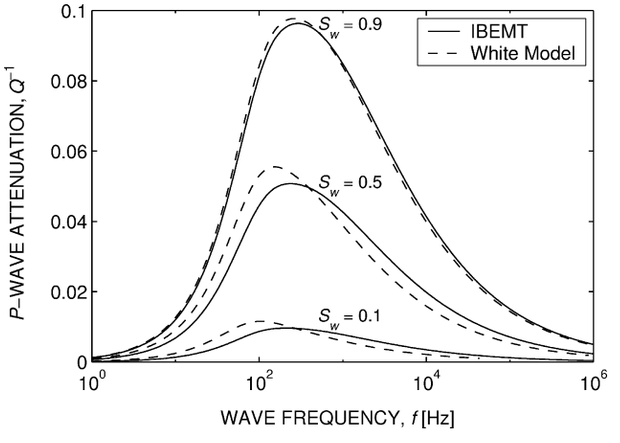

FIG. 5. Same as Figure 4, except results are shown for P-wave attenuation instead of P-wave velocity.

frequencies (where the standard IBEMT formulation has previously been inapplicable), our predictions agree very closely with the corrected White model (White, 1975; Dutta and Seriff, 1979). We therefore conclude that our approach is a generalization and embedding of the White model into the inclusion-based framework.

The key benefit of our approach is that it extends IBEMT to model elastic wave velocities and dispersion in the intermediate frequency regime. This is a significant contribution to the inclusion-based modeling paradigm, the versatility of which allows one to model diverse phenomena arising from heterogeneity. For example, we have illustrated how our approach can model frequency-dependent behavior of media in which patches of multiple sizes are simultaneously present. Similarly, porous media containing additional solid or fluid phases are easily accommodated. Patches having other than spherical geometry (e.g., ellipsoidal patches), and even multiple patches having different geometries, could also be treated within this framework, by deriving expressions for the complex moduli of patches of different shapes. In contrast, the White model does not easily permit these generalizations.

The chief limitation of the model presented here is that we consider saturation heterogeneity at the patch scale only, effectively neglecting pore-scale effects. This limitation (which is shared by the White model, and all other models) is serious, since we expect that saturation heterogeneity, in most realistic porous materials, will exist at many length scales ranging from micrometers to kilometers. In order to accurately model and interpret measurements of elastic wave velocities, the effect of heterogeneity at all of these scales needs to be accounted for. This is a significant challenge that requires that we continue to improve our ability to model the complex scale-dependent heterogeneity of natural geologic systems.

ACKNOWLEDGMENTS

This research was supported by an NSERC Industrially-Oriented Research Grant to Rosemary Knight with funding from Imperial Oil, Petro-Canada, and Western Atlas. Richard Taylor was also supported in part by a University Graduate Fellowship from the University of British Columbia.

REFERENCES

Berryman, J. G., 1980a, Long-wavelength propagation in composite elastic media. I. Spherical inclusions: J. Acoust. Soc. Am., **68**, 1809–1819.

——— 1980b, Long-wavelength propagation in composite elastic media. II. Ellipsoidal inclusions: J. Acoust. Soc. Am., **68**, no. 6, 1820–1831.

Biot, M. A., 1956, Theory of propagation of elastic waves in a fluid-saturated porous solid. I. Low-frequency range: J. Acoust. Soc. Am., **28**, 168–178.

Cadoret, T., Marion, D., and Zinszner, B., 1995, Influence of frequency and fluid distribution on elastic wave velocities in partially saturated limestones: J. Geophys. Res., **100**, 9789–9803.

Domenico, S. N., 1977, Elastic properties of unconsolidated sand reservoirs: Geophysics, **42**, 1339–1368.

Dutta, N. C., and Odé, H., 1979, Attenuation and dispersion of compressional waves in fluid-filled porous rocks with partial gas saturation (White model)—Part I: Biot Theory, Part II: Results: Geophysics, **44**, 1777–1805.

Dutta, N. C., and Seriff, A. J., 1979, On White's model of attenuation in rocks with partial gas saturation: Geophysics, **44**, 1806–1812.

Dvorkin, J., Nolen-Hoeksema, R., and Nur, A., 1994, The squirt flow mechanism: Macroscopic description: Geophysics, **59**, 428–438.

Endres, A. L., and Knight, R. J., 1989, The effect of microscopic fluid distribution on elastic wave velocities: The Log Analyst, **30**, 437–445.

Gassmann, F., 1951, Über die elastizität poröser medien: Vierteljahrsschrift der Naturforschenden Gesellschaft in Zürich, **96**, 1–23.

Gist, G. A., 1994, Interpreting laboratory velocity measurements in partially gas-saturated rocks: Geophysics, **59**, 1100–1109.

Guéguen, Y., and Palciauskas, V., 1994, Introduction to the physics of rocks: Princeton Univ. Press.

Knight, R., Dvorkin, J., and Nur, A., 1998, Acoustic signatures of partial saturation: Geophysics, **63**, 132–138.

Knight, R., and Nolen-Hoeksema, R., 1990, A laboratory study of the dependence of elastic wave velocities on pore scale fluid distribution: Geophys. Res. Lett., **17**, 1529–1532.

le Ravalec, M., and Guéguen, Y., 1996, High- and low-frequency elastic moduli for a saturated porous/cracked rock—Differential self-consistent and poroelastic theories: Geophysics, **61**, 1080–1094.

le Ravalec, M., Guéguen, Y., and Chelidze, T., 1996, Elastic wave velocities in partially saturated rocks: Saturation hysteresis: J. Geophys. Res., **101**, no. B1, 837–844.

Mavko, G., Mukerji, T., and Dvorkin, J., 1998, The rock physics handbook: Cambridge Univ. Press.

Nur, A., and Byerlee, J. D., 1971, An exact effective stress law for elastic deformation of rocks with fluids: J. Geophys. Res., **76**, 6414–6419.

White, J. E., 1975, Computed seismic speeds and attenuation in rocks with partial gas saturation: Geophysics, **40**, 224–232.

APPENDIX A

PRESSURE DIFFUSION EQUATIONS

Here, we derive partial differential equations describing the diffusion of fluid pressure in a porous medium. In a sample of fluid-saturated porous medium, we consider a region of volume V within which the medium is homogeneous, in that the induced fluid pressure is spatially uniform when a uniform pressure p is applied at the region's boundary. Under this assumption, Guéguen and Palciauskas (1994) [following Nur and Byerlee (1971)] derive the "constitutive relation of poroelasticity,"

$$p - \alpha p_f = -\kappa_d \theta, \tag{A-1}$$

where p_f is the induced fluid pressure and θ is the volumetric dilatation of the region. Here, κ_d is the dry frame bulk modulus, and $\alpha = 1 - \kappa_d/\kappa_s$, where κ_s is the bulk modulus of the mineral solid.

The volumetric average,

$$\theta = \phi\theta_f + (1-\phi)\theta_s, \tag{A-2}$$

can be used to express the overall dilatation θ in terms of the individual dilatations θ_f and θ_s of the fluid and solid components, respectively, where ϕ is the porosity. Assuming that the fraction of the region's boundary occupied by the fluid phase is identical to the porosity [this assumption is discussed in Biot (1956)], the same average can be used to relate the pressure at the region's boundary to the pressures p_f and p_s in the individual components, i.e.,

$$p = \phi p_f + (1-\phi)p_s. \tag{A-3}$$

Since the solid component is subject to a homogeneous pressure due to the pore fluid, the constitutive elastic relation for

the solid component is given by

$$p_s = -\kappa_s \theta_s. \tag{A-4}$$

The elastic relation for the fluid is

$$\frac{dp_f}{dt} = -\kappa_f \frac{d\theta_f}{dt} - \frac{\kappa_f Q}{\phi V}, \tag{A-5}$$

where κ_f is the bulk modulus of the fluid. Here, Q represents the volume rate of fluid flow out through the region's boundary. We use Darcy's law $\mathbf{v} = -K/\eta \nabla p_f$ to express the volume-averaged flow rate, $\mathbf{v}$, in terms of the permeability, K, and the viscosity, η. Since the region V is arbitrary, equation (A-5) yields

$$\frac{\partial p_f}{\partial t} = -\kappa_f \frac{\partial \theta_f}{\partial t} + \frac{\kappa_f K}{\phi \eta} \nabla^2 p_f. \tag{A-6}$$

This is equivalent to equation (C-8) of White (1975), with the addition of a forcing term.

If we assume that the pressure field p is known, we can write equation (A-6) in terms of p [using relations (A-1) through (A-4)] to yield

$$\frac{\partial p_f}{\partial t} = D_p \nabla^2 p_f + \frac{\alpha F_p}{\phi \kappa_d} \frac{\partial p}{\partial t}, \tag{A-7}$$

where the parameters D_p and F_p are given by

$$D_p = \frac{K F_p}{\phi \eta}, \tag{A-8}$$

$$\frac{1}{F_p} = \frac{1}{\kappa_f} - \frac{1}{\kappa_s} + \frac{\alpha}{\phi \kappa_d}. \tag{A-9}$$

APPENDIX B

EFFECTIVE BULK MODULUS OF A SPHERICAL PATCH

We consider a fluid-saturated, porous spherical patch of radius a, embedded at the center of a background medium of radius b (see Figure 1). Since we regard the uniform pressure field p as prescribed, we use equation (A-7) to describe the evolution of the fluid pressure in the sample. Defining the dimensionless radius $\hat{r} = r/a$, writing $p = p_0 e^{i\omega t}$ and $p_f = p_f(\hat{r}) e^{i\omega t}$, and exploiting spherical symmetry, we obtain

$$i\omega p_f(\hat{r}) = \frac{D_{p(i)}}{a^2} \frac{1}{\hat{r}^2} \frac{d}{d\hat{r}} \left(\hat{r}^2 \frac{dp_f(\hat{r})}{d\hat{r}} \right) + i\omega \frac{\alpha_i F_{p(i)}}{\phi_i \kappa_{d(i)}} p_0, \tag{B-1}$$

where the subscript $i = 1$ for $\hat{r} < a$ (inside the patch) and $i = 2$ for $\hat{r} > a$ (outside the patch). The function $p_f(\hat{r})$ is constrained to satisfy the following conditions:

$$p_f'(0) = p_f'(R) = 0, \tag{B-2}$$

with $R = b/a$ (i.e., no flow at the endpoint $r = 0$ or the boundary $r = b$),

$$p_f(1^-) = p_f(1^+) \tag{B-3}$$

(i.e., continuity of the pressure field at $r = a$), and

$$Z_1 p_f'(1^-) = Z_2 p_f'(1^+), \tag{B-4}$$

with $Z_i = K_i/\eta_i$ (i.e., continuity of the fluid flux at $r = a$).

The volumetric dilatation field inside the patch can be written, using the poroelastic relation (A-1), as

$$\theta(\hat{r}) = -\frac{p_0 - \alpha_1 p_f(\hat{r})}{\kappa_{d(1)}} = -\frac{p_0}{\kappa_{d(1)}} \left(1 - \alpha_1 \frac{p_f(\hat{r})}{p_0} \right). \tag{B-5}$$

Thus the total dilatation of the patch, θ_0, which is the average of $\theta(\hat{r})$ over the patch, is given by

$$\begin{aligned} \theta_0 &= \int_0^1 \hat{r}^2 \theta(\hat{r}) d\hat{r} \\ &= -\frac{p_0}{\kappa_{d(1)}} \left(1 - \alpha_1 \int_0^1 3\hat{r}^2 \frac{p_f(\hat{r})}{p_0} d\hat{r} \right). \end{aligned} \tag{B-6}$$

Relating the total dilatation of the patch to the applied pressure defines the effective bulk modulus, κ^*, via the relation

$$p_0 = -\kappa^* \theta_0. \tag{B-7}$$

We obtain, after solving equation (B-1) subject to the constraints (B-2) through (B-4) and simplifying,

$$\kappa^* = \frac{\kappa_{d(1)}}{1 - \alpha_1 [G_1 + F(\omega)(G_2 - G_1)]}, \tag{B-8}$$

with dimensionless parameters

$$\varphi_i = \sqrt{\frac{i\omega a^2}{D_{p(i)}}}, \quad G_i = \frac{\alpha_i F_{p(i)}}{\phi_i \kappa_{d(i)}}, \tag{B-9}$$

and

$$F(\omega) = \frac{3}{\varphi_1^2} \frac{A_1 A_2}{A_3 + A_4}, \tag{B-10}$$

$$A_1 = (1 - \varphi_1) - (1 + \varphi_1) e^{-2\varphi_1}, \tag{B-11}$$

$$A_2 = M_1 + M_2 e^{-2\varphi_3}, \tag{B-12}$$

$$A_3 = (1 - R\varphi_2)\left(M_3 + M_4 e^{-2\varphi_1} \right), \tag{B-13}$$

$$A_4 = (1 + R\varphi_2)\left(M_5 + M_6 e^{-2\varphi_1} \right) e^{-2\varphi_3}, \tag{B-14}$$

$$\varphi_3 = (R - 1)\varphi_2 = \sqrt{\frac{i\omega(b - a)^2}{D_{p(2)}}}, \tag{B-15}$$

$$M_1 = \varphi_3 - R\varphi_2^2 + 1, \tag{B-16}$$

$$M_2 = \varphi_3 + R\varphi_2^2 - 1, \tag{B-17}$$

$$M_3 = -1 - \varphi_1 B + B - \varphi_2, \tag{B-18}$$

$$M_4 = 1 - \varphi_1 B - B + \varphi_2, \tag{B-19}$$

$$M_5 = 1 + \varphi_1 B - B - \varphi_2, \tag{B-20}$$

$$M_6 = -1 + \varphi_1 B + B + \varphi_2, \tag{B-21}$$

$$B = Z_1/Z_2. \tag{B-22}$$